

## E. García-Hemme, K. M. Yu, P. Wahnou, G. González-Díaz, and W. Walukiewicz

View online: <http://dx.doi.org/10.1063/1.4919791>Published by the [AIP Publishing](#)

### Correlation of spectral features of photoluminescence with residual native defects of ZnO thin films annealed at different temperatures

### Effect of annealing on the microstructure and optical properties of ZnO / V<sub>2</sub>O<sub>5</sub> composite

## Study of the photoluminescence of phosphorus-doped p -type ZnO thin films grown by radio-frequency magnetron sputtering

## Identification of nitrogen chemical states in N -doped ZnO via x-ray photoelectron spectroscopy

### Photoluminescence dependence of ZnO films grown on Si(100) by radio-frequency magnetron sputtering on the growth ambient

Appl. Phys. Lett. **82**, 2625 (2003); 10.1063/1.1568543



# Effects of the d-donor level of vanadium on the properties of $\text{Zn}_{1-x}\text{V}_x\text{O}$ films

E. García-Hemme,<sup>1,2,3,a)</sup> K. M. Yu,<sup>3,4</sup> P. Wahnon,<sup>2,5</sup> G. González-Díaz,<sup>1,2</sup>  
 and W. Walukiewicz<sup>3</sup>

<sup>1</sup>*Dpto. de Física Aplicada III (Electricidad y Electrónica), Univ. Complutense de Madrid, Madrid 28040, Spain*

<sup>2</sup>*CEI Campus Moncloa, UCM-UPM, Madrid 28040, Spain*

<sup>3</sup>*Materials Sciences Division, Lawrence Berkeley National Laboratory, 1 Cyclotron Road, Berkeley, California 94720, USA*

<sup>4</sup>*Department of Physics and Materials Science, City University of Hong Kong, Kowloon, Hong Kong*

<sup>5</sup>*Instituto de Energía Solar and Depto TFB, E.T.S.I. Telecomunicación, Univ. Politécnica de Madrid, Ciudad Universitaria, Madrid 28040, Spain*

(Received 24 February 2015; accepted 24 April 2015; published online 5 May 2015)

We report the effect of d-levels of vanadium atoms on the electronic band structure of ZnO. Polycrystalline layers of  $\text{Zn}_{1-x}\text{V}_x\text{O}$  with  $0 \leq x \leq 0.08$  were synthesized using magnetron sputtering technique. Electrical measurements show that electron concentration increases with vanadium up to  $x = 0.04$  and then decreases and films become insulating for  $x > 0.06$ . Optical characterization reveals that the absorption edge shifts to higher energy, while the photoluminescence (PL) peak shows a shift to lower energy with increasing vanadium content. This unusual optical behavior can be explained by an anticrossing interaction between the vanadium d-levels and the conduction band (CB) of ZnO. The interaction results in an upward shift of unoccupied CB ( $E_+$ ) and the downward shift of the fully occupied  $E_-$  band derived from the vanadium d-levels. The composition dependence of optical absorption edge ( $E_+$ ) and PL peak ( $E_-$ ) can be fitted using the Band Anticrossing model with the vanadium d-level located at 0.13 eV below CB of ZnO and a coupling constant of 0.65 eV. © 2015 AIP Publishing LLC. [<http://dx.doi.org/10.1063/1.4919791>]

Zinc oxide (ZnO) is a wide gap semiconductor that has been extensively studied for potential applications as light emitters,<sup>1</sup> field effect transistors,<sup>2</sup> or as transparent conductors.<sup>3</sup> As grown ZnO is typically n-type, while p-type doping of ZnO is still challenging.<sup>4,5</sup> This asymmetry in the doping behavior can be attributed to a large electron affinity of ZnO of about 4.6–4.8 eV.

Increasing the n-type conductivity of ZnO is usually achieved by doping with a group III element (such as Al, Ga, or In). In fact, Al (AZO) and Ga (GZO) doped ZnO can have resistivities  $\sim 10^{-4} \Omega\text{-cm}$ , making them good candidates to replace tin doped indium oxide (ITO) as transparent conductors for photovoltaics.<sup>3</sup> Group 3-d transition metals (TMs) with  $4s^23d^n$  (or  $4s^13d^n$  for Cr and Cu) electronic configuration, where  $n$  is the number of 3d electrons, are isovalent when substituting cations in the group II–VI compounds. However, the substitutional TM ions can also act as dopants through the charge transfer between partially filled d-shells and the extended bands of the crystal. The energies of the localized d-donor and d-acceptor states in II–VI compounds were compiled in Ref. 6. It was shown that because of their localized nature, the d-shell derived states remain constant on the absolute scale relative to the vacuum level. This allows prediction of the energy of the d-states from the known band offsets between different II–VI semiconductors. Vanadium atoms substituting cations in II–VI semiconductors form a localized d-donor levels about 5 eV below the vacuum level.<sup>7</sup> Therefore, V on Zn site will form a donor level slightly below the conduction band edge (CBE) of ZnO, whose electron affinity is about 4.8 eV.<sup>8</sup> Previous reports on vanadium doped

ZnO mainly focused on ferromagnetic properties for possible spintronic applications.<sup>9</sup> In this paper, we study the electrical and optical properties of  $\text{Zn}_x\text{V}_{1-x}\text{O}$  thin films with  $0 \leq x \leq 0.08$ . The results are analyzed within the framework of the Band Anticrossing (BAC) model considering the interaction of the localized d-levels of vanadium atoms with the extended states of the ZnO conduction band.

We have synthesized  $\text{Zn}_{1-x}\text{V}_x\text{O}$  thin films with  $0 \leq x \leq 0.08$  using radio frequency magnetron sputtering. Polycrystalline ZnO:V films were deposited on glass substrates at 250 °C. Two separate sputtering targets were used, a ZnO target and a  $\text{V}_2\text{O}_3$  target, and the composition was controlled by varying the sputtering power and target to substrate distance of the individual target. Argon pressure of  $\sim 5$  mTorr was maintained during sputtering. Film thickness and composition were determined by Rutherford Backscattering Spectrometry (RBS) using a 3 MeV alpha particle beam at a backscattered angle of 165°. Resistivity, mobility, and free carrier concentration measurements were carried out using an Ecopia HMS-3000 Hall measurement system in the van der Pauw configuration with a magnetic field 0.6 T.

Transmittance and reflectance measurements were carried out using a Perkin-Elmer Lambda 950 spectrophotometer working with a Universal Reflectance Accessory. For photoluminescence (PL) measurements, the 325 nm line of a He-Cd laser working at 50 mW was used as the excitation source. Emission spectra were collected with a SPEX-1404 0.85 m double spectrometer and a photomultiplier tube detector (Hamamatsu R928 photomultiplier) working at room-temperature.

Figure 1 shows the room-temperature electron concentration and mobility as a function of the vanadium content. The pure ZnO thin film was insulating probably due to close

<sup>a)</sup>E-mail: eric.garcia@ucm.es

to stoichiometric (or slightly O-rich) composition. As is seen in Fig. 1, the  $\text{Zn}_{1-x}\text{V}_x\text{O}$  films become conductive for  $x \geq 0.03$  and both electron concentration and mobility reach maximum values for  $x = 0.04$ . The resistivity of alloy films are not measurable ( $\rho > 1000 \Omega\text{-cm}$ ) for V content larger than  $x = 0.06$ . The decrease of electron concentration and mobility at high V content are likely due to the degradation of film crystallinity and an increase in the formation of compensating defects in the films. This degradation of film crystallinity for V content higher than  $x = 0.043$  has been already observed in Ref. 10 using scanning electron microscopy. A lower crystal quality for high vanadium content has been also observed using X ray diffraction in  $\text{ZnVO}$  grown by pulsed laser deposition<sup>11</sup> as well as in vanadium doped  $\text{ZnO}$  prepared by the sprayed pyrolysis technique.<sup>12</sup> It is evident from the data that V on Zn site acts as a donor contributing electron from highly localized d-level. Based on Ref. 6, vanadium substituting Zn site in  $\text{ZnO}$  is expected to have a donor level associated with the  $3d^3$  to  $3d^2$  charge transition state located slightly below the conduction band edge of  $\text{ZnO}$  matrix. The electrons transferred from the d-level are responsible for the n-type conductivity in  $\text{Zn}_{1-x}\text{V}_x\text{O}$ , as shown in Fig. 1.

In order to better understand the effect of the localized d-states on the electronic structure of the conduction band of  $\text{ZnO}$ , we have measured optical absorption and photoluminescence in  $\text{Zn}_{1-x}\text{V}_x\text{O}$  films with composition  $x$  up to 0.06. The absorption coefficients were deduced from transmittance and reflectance measurements. Figure 2 shows the absorption coefficient squared ( $\alpha^2$ ) as a function of the photon energy. Film thickness as determined by RBS was typically about  $\sim 180$  nm. The films showed a clear monotonous blue shift of the absorption edge with increasing V content. This behavior has been previously observed in epitaxial  $\text{Zn}_{1-x}\text{V}_x\text{O}$  layers grown on sapphire substrates using pulsed laser deposition.<sup>13</sup> The absorption edge shift cannot be attributed to the Burstein-Moss shift, since for more than  $x = 0.04$  V, the charge concentration is decreasing with increasing V content. Also this upward shift in absorption edge cannot be explained by alloying with different vanadium oxides phases ( $\text{VO}$ ,  $\text{V}_2\text{O}_3$ , and  $\text{V}_2\text{O}_5$ ), whose band gap energies range from 2.2 to 2.7 eV.<sup>14,15</sup>

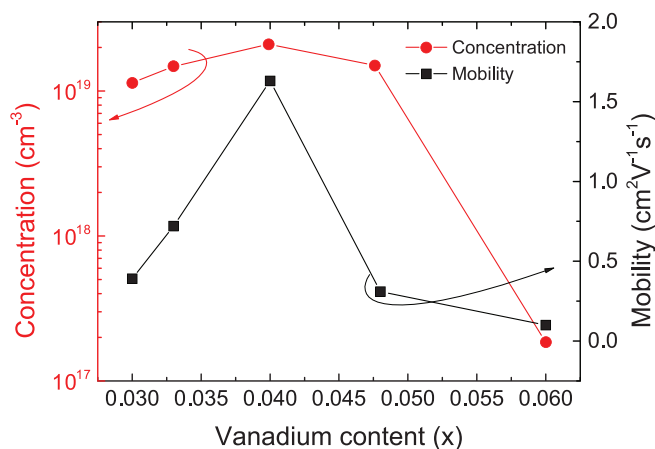


FIG. 1. Room temperature charge carriers concentration (left axis, red circles) and mobility (right axis, black squares) as a function of the vanadium content  $x$ .

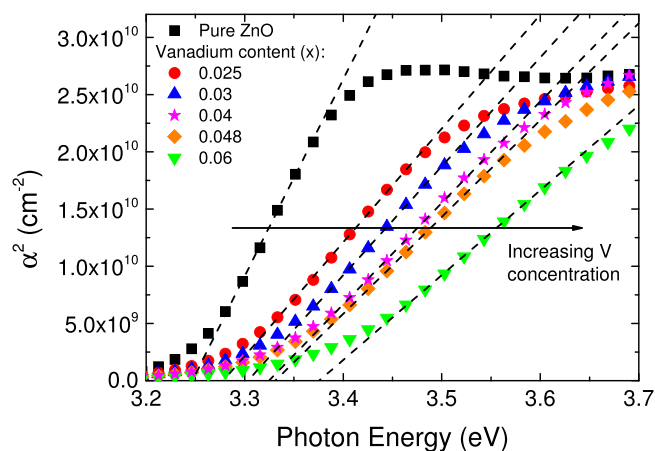


FIG. 2. Spectral room-temperature absorption coefficient squared for the pure  $\text{ZnO}$  sample and a representative set of  $\text{Zn}_{1-x}\text{V}_x\text{O}$  samples with different vanadium contents. Remark the clear absorption edge shift towards higher photons energies as the vanadium content increases in the layers.

Figure 3(a) shows photoluminescence spectra for samples with different vanadium concentrations. A strong initial red-shift of the emission peak by  $\sim 150$  meV for the sample with  $x = 0.025$  is observed. As the V content further increases in the film, the PL energy decreases much more slowly. The increased linewidth and an asymmetric shape of the luminescence peaks for the  $\text{ZnVO}$  samples suggest that there is more than one emission contributing to the PL. We fitted all the peaks in Fig. 3(a) using two emission lines. An example of the fitting procedure is shown in Fig. 3(b) for the sample with  $x = 0.048$ . The composition dependence of the energies of the low and high energy peaks obtained from the fitting procedure is shown in Fig. 3(c). The emission energy of the high energy peak remains almost constant at  $\sim 3.22$  eV, whereas the low energy peak red-shifts from 3.08 eV to 3.00 eV with increasing vanadium content. Since the high energy peak position remains constant at  $\sim 3.22$  eV for all V composition, and that it is close to the bandgap energy of pure  $\text{ZnO}$ , we attribute this PL peak to small  $\text{ZnO}$  crystals present in the films that is not detectable in the absorption spectra, whereas the lower energy PL peak can be attributed to the emission from the  $\text{Zn}_{1-x}\text{V}_x\text{O}$  alloy. This downward shift in the low energy PL peak is in striking contrast to the upward shift observed in the absorption edge, as shown in Fig. 2.

Figure 4 shows the absorption edge energy and the low energy emission peak position as a function of the vanadium content. Absorption edge energy was determined by extrapolating  $\alpha^2$ , as shown in Fig. 2, to the base line. The results in Fig. 4 clearly show an opposite trend for the PL and absorption data, the absorption edge energy increases, while the PL peak shifts to lower energies with increasing V content.

The unusual electrical and optical properties of  $\text{ZnVO}$  can be explained by an interaction between localized d-states of V and the extended states of the  $\text{ZnO}$  matrix. When large enough concentration of substitutional V is incorporated, the localized d-states form a band through the interaction with the conduction band of  $\text{ZnO}$ . In order to describe this interaction, we adopt the BAC model<sup>16–18</sup> that has been used to describe electronic band structure of Highly Mismatched Alloys (HMAs), in which metallic atoms are partially



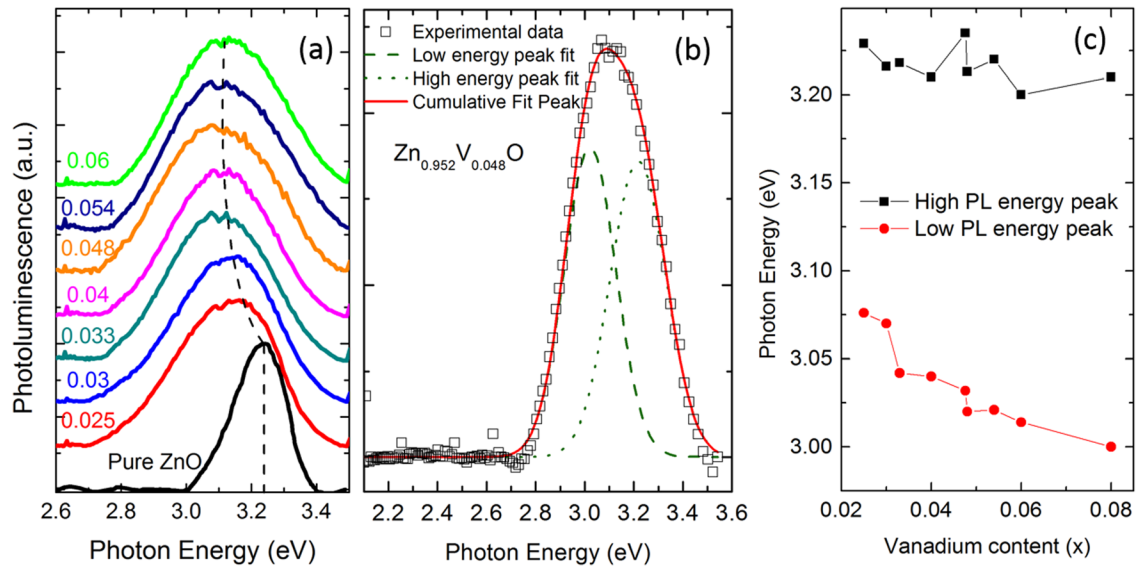


FIG. 3. (a) Room-temperature photoluminescence spectra for the pure ZnO sample and a representative set of  $\text{Zn}_{1-x}\text{V}_x\text{O}$  samples with different vanadium contents. Vertical dashed line represents the peak energy position for each sample. (b) De-convolution process accomplished on the emission spectra. Example with the sample that presents an  $x = 0.048$  of vanadium showing two emission peaks. (c) High energy emission peak and low energy emission peak energetic positions as a function of the vanadium content.

replaced with more electronegative atoms. The strength of the anticrossing interaction depends on the degree of the mismatch between substitutional atoms and the energy separation between the localized states and the CBE. As the result of BAC interaction, two sets of states are formed with the dispersion relations given by

$$E_{\pm} = \frac{1}{2} \left( E_C(k) + E_d \pm \left[ (E_C(k) - E_d)^2 + 4C^2x \right]^{1/2} \right), \quad (1)$$

where  $E_C(k)$  is the dispersion relation of the ZnO conduction band  $E_d$  is the vanadium d-level energy,  $x$  is the vanadium content, and  $C$  is the matrix element describing the coupling between localized states and the extended states.<sup>17,19</sup>

There is an important difference between BAC in standard III-V or II-VI HMA and  $\text{Zn}_{1-x}\text{V}_x\text{O}$ . In the former, the BAC interaction occurs between states of the same

symmetry, e.g., in dilute III-V nitrides the localized s-like states of N interact with extended s-like conduction band states of the host matrix. In contrast, in ZnVO alloys, the localized d-level donor states of V interact with the s-like conduction band states of ZnO. Therefore, substitution of N for a group V element in III-N-V alloys does not change the total number of the conduction band states, whereas replacing Zn with dilute amount of V adds the V d-donor states to the total number of conduction band states. This difference is important for a quantitative description of any effects dependent on the total density of states, however, it does not affect the dispersion relations and thus also energies of the optical transitions that are analyzed in this work.

Vanadium substituting Zn in ZnO has the charge transition state  $3d^3$  to  $3d^2$  at about 0.13 eV below the CBE of ZnO. This means that one of the three 3d electrons can be excited to the CBE. At high enough V content, the BAC interaction of the 3d states with the CB states leads to the formation of the V d-state derived  $E_-$  subband and CB derived  $E_+$  subband. States in both bands are broadened with the largest broadening for the states with energy closest to the localized 3d donor state. The broadening leads to an overlap between fully occupied  $E_-$  and an empty  $E_+$  band with the Fermi energy located in the range of heavily broadened states between  $E_-$  and  $E_+$ . The broadening of the states at the Fermi energy is responsible for the very small electron mobility observed in  $\text{Zn}_{1-x}\text{V}_x\text{O}$ . Therefore, since the narrow  $E_-$  band is occupied, the absorption edge is associated with transitions from the valence band edge (VBE) to unoccupied  $E_+$  band, whereas the emission originates from transitions between occupied  $E_-$  band and the VBE. We have used Eq. (1) to fit the data presented in Fig. 4. The solid lines represent the best fit that was obtained with  $E_d = 3.12$  eV and  $C = 0.65$ .

Figure 5 shows an example of the dispersion relations for the  $E_-(k)$  and  $E_+(k)$  subbands calculated for  $\text{Zn}_{0.96}\text{V}_{0.04}\text{O}$  using Eq. (1).  $E_C(k)$  and  $E_V(k)$  represent, respectively, the

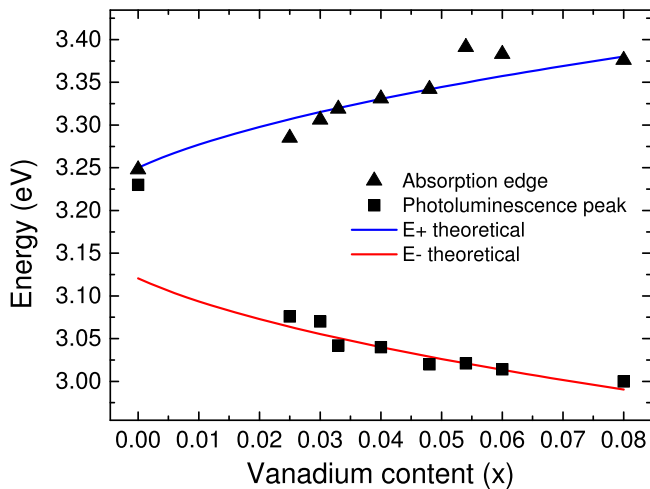


FIG. 4. Band edge energies (extracted from fitting to  $\alpha^2$  vs photon energies) in triangles symbols and low emission peak energy position in square symbols as a function of the vanadium content. Solid lines represent fitting results of the BAC model for the  $E_+$  and  $E_-$  sub-bands.

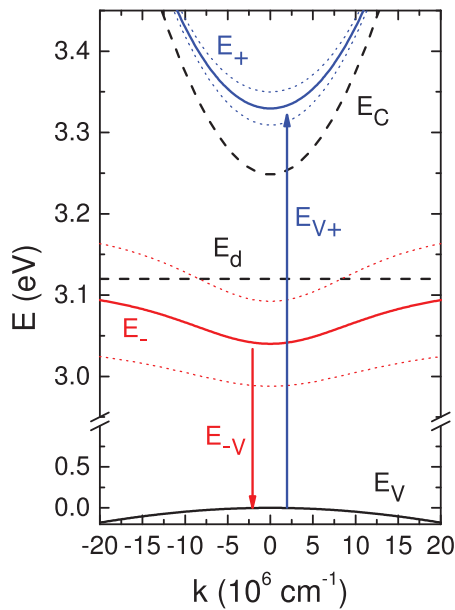


FIG. 5. The calculated band structure for  $\text{Zn}_{1-x}\text{V}_x\text{O}$  with  $x \sim 0.04$ .  $E_{-V}$  represent transitions from the  $E_{-}$  sub-band to the VB and are the main origin of the photoluminescence spectra, while  $E_{V+}$  represent transitions from the VB to the  $E_{+}$  sub-band which are responsible for the absorption measurements. Dotted lines represent broadening of the dispersion curves of the newly formed sub-bands illustrating the energy uncertainties defined in Eq. (2).

conduction and valence band for ZnO host matrix, while  $E_d$  is the localized vanadium d-level located at 3.12 eV above VBE or 0.13 eV below the CBE of ZnO matrix. The dispersion relations shown in Fig. 5 assume broadening of the electronic states. The broadening of the  $E_{-}$  and  $E_{+}$  bands originates from homogeneous broadening from the finite lifetime of interacting electronic states and possible inhomogeneous broadening from nonrandom fluctuations of the spatial distribution of V atoms in the crystal. The homogeneous broadening, that is an inherent part of the BAC model, is proportional to the admixture of the localized V state wavefunction. The broadening of the  $E_{-}(k)$  or  $E_{+}(k)$  states is given by

$$\Gamma_{\pm}(k) = \Gamma_L \frac{[E_{\pm}(k) - E_C(k)]}{[E_{\pm}(k) - E_C(k)] + [E_{\pm}(k) - E_d]}, \quad (2)$$

where  $\Gamma_L$  represents the broadening of the V level in one impurity level Anderson model.<sup>20</sup> It is seen that the maximum broadening is found for  $E_{-}$  or  $E_{+}$  approaching the localized V level.<sup>17</sup> This, as is shown in Fig. 5, happens for  $k = 0$  for  $E_{+}$  and very large  $k$  for  $E_{-}$ .

In the case of ZnVO,  $E_{-}$  level is fully occupied and the Fermi energy falls into the energy region with the large broadening which strongly affects electrical and optical properties of the material. In addition, the broadening introduces small density of states into the energy gap between  $E_{-}$  and  $E_{+}$  bands. This explains the change in the slope of the absorption edge, as shown in Fig. 2. The large broadening of the final states for the optical transitions from the valence band to the conduction band relaxes the wavevector selection rules and leads to a diffuse absorption edge. The broadening effects are increasing with increasing V content.

In conclusions,  $\text{Zn}_{1-x}\text{V}_x\text{O}$  polycrystalline thin films with vanadium content  $0 < x < 0.08$  have been synthesized

by means of RF magnetron sputtering technique. Spectral absorption coefficient results showed that the absorption edge moves towards higher energy as the vanadium content increases. In contrast, PL measurements showed an opposite trend with the PL peak energy shifting down with increasing V concentration. We used the BAC model to describe an interaction between the localized d-levels of V atoms and the extended states of the ZnO CB. Such interaction results in an upward shift of the mostly unoccupied conduction band states ( $E_{+}$  sub-band) and broadening of the occupied V donor d-levels into a narrow band ( $E_{-}$  sub-band). The vanadium d-level position at 0.13 eV below CB minimum and the coupling parameter of the interaction of 0.65 eV were obtained from fitting the experimental absorption and PL data using the BAC model.

This work was supported by the Director, Office of Science, Office of Basic Energy Sciences, Materials Sciences and Engineering Division and National Center for Electron Microscopy/LBNL, under Contract No. DE-AC02-05CH11231. This work was partially supported by the Project MADRID-PV (P 2013/MAE-2780) funded by the Comunidad de Madrid and the project TEC 2013-41730-R and ENE2013-46624-C4-2 from the Spanish MINECO. E. García-Hemme acknowledges the support by a PICATA Predoctoral Fellowship of the Moncloa Campus of International Excellence (UCM-UPM).

- <sup>1</sup>J. H. Lim, C. K. Kang, K. K. Kim, I. K. Park, D. K. Hwang, and S. J. Park, *Adv. Mater.* **18**(20), 2720 (2006).
- <sup>2</sup>K. Nomura, H. Ohta, K. Ueda, T. Kamiya, M. Hirano, and H. Hosono, *Science* **300**(5623), 1269–1272 (2003).
- <sup>3</sup>T. Minami, *Semicond. Sci. Technol.* **20**(4), S35–S44 (2005).
- <sup>4</sup>D. C. Look, D. C. Reynolds, C. W. Litton, R. L. Jones, D. B. Eason, and G. Cantwell, *Appl. Phys. Lett.* **81**(10), 1830–1832 (2002).
- <sup>5</sup>K. K. Kim, H. S. Kim, D. K. Hwang, J. H. Lim, and S. J. Park, *Appl. Phys. Lett.* **83**(1), 63–65 (2003).
- <sup>6</sup>J. M. Langer, C. Delerue, M. Lannoo, and H. Heinrich, *Phys. Rev. B* **38**(11), 7723–7739 (1988).
- <sup>7</sup>C. J. Vesely and D. W. Langer, *Phys. Rev. B* **4**(2), 451 (1971).
- <sup>8</sup>U. Ozgur, Y. I. Alivov, C. Liu, A. Teke, M. A. Reshchikov, S. Dogan, V. Avrutin, S. J. Cho, and H. Morkoc, *J. Appl. Phys.* **98**(4), 041301 (2005).
- <sup>9</sup>H. Saeki, H. Tabata, and T. Kawai, *Solid State Commun.* **120**(11), 439–443 (2001).
- <sup>10</sup>J. T. Luo, X. Y. Zhu, B. Fan, F. Zeng, and F. Pan, *J. Phys. D: Appl. Phys.* **42**(11), 115109 (2009).
- <sup>11</sup>M. E. Koleva, P. A. Atanasov, N. N. Nedialkov, H. Fukuoka, and M. Obara, *Appl. Surf. Sci.* **254**(4), 1228–1231 (2007).
- <sup>12</sup>A. Mhamdi, A. Boukhachem, M. Madani, H. Lachheb, K. Boubaker, A. Amlouk, and M. Amlouk, *Optik* **124**(18), 3764–3770 (2013).
- <sup>13</sup>S. Ramachandran, A. Tiwari, J. Narayan, and J. T. Prater, *Appl. Phys. Lett.* **87**(17), 172502 (2005).
- <sup>14</sup>W. T. Liu, J. Cao, W. Fan, Z. Hao, M. C. Martin, Y. R. Shen, J. Wu, and F. Wang, *Nano Lett.* **11**(2), 466–470 (2011).
- <sup>15</sup>T. Zhai, H. Liu, H. Li, X. Fang, M. Liao, L. Li, H. Zhou, Y. Koide, Y. Bando, and D. Goberg, *Adv. Mater.* **22**(23), 2547–2552 (2010).
- <sup>16</sup>W. Shan, W. Walukiewicz, J. W. Ager, E. E. Haller, J. F. Geisz, D. J. Friedman, J. M. Olson, and S. R. Kurtz, *Phys. Rev. Lett.* **82**(6), 1221–1224 (1999).
- <sup>17</sup>J. Wu, W. Shan, and W. Walukiewicz, *Semicond. Sci. Technol.* **17**(8), 860–869 (2002).
- <sup>18</sup>N. Lopez, L. A. Reichertz, K. M. Yu, K. Campman, and W. Walukiewicz, *Phys. Rev. Lett.* **106**(2), 028701 (2011).
- <sup>19</sup>W. Walukiewicz, W. Shan, K. M. Yu, J. W. Ager, E. E. Haller, I. Miotkowski, M. J. Seong, H. Alawadhi, and A. K. Ramdas, *Phys. Rev. Lett.* **85**(7), 1552–1555 (2000).
- <sup>20</sup>P. W. Anderson, *Phys. Rev.* **124**(1), 41 (1961).